MAGNETOHYDRODYNAMICS Vol. 55 (2019), No. 1-2, pp. 225–231
DOI: 10.22364/mhd.55.1-2.27

CROSS HELICITY SIGN REVERSALS IN THE DISSIPATIVE SCALES OF MAGNETOHYDRODYNAMIC TURBULENCE

V. Titov[1], *R. Stepanov*[1], *N. Yokoi*[2], *M. Verma*[3], *R. Samtaney*[4]

[1] *Institute of Continuous Media Mechanics, Perm 614013, Russia*
[2] *Institute of Industrial Science University of Tokyo, Tokyo 153-8505, Japan*
[3] *Department of Physics, Indian Institute of Technology Kanpur, Kanpur 20816, India*
[4] *Mechanical Engineering, Division of Physical Science and Engineering, King Abdullah University of Science and Technology, Thuwal 23955-6900, Kingdom of Saudi Arabia*

Direct numerical simulations of magnetohydrodynamic turbulence with kinetic energy and cross helicity injections at large scales are performed. It was observed that cross helicity changes its sign as we go from large and intermediate scales to small scales. In addition, the magnetic reconnections are strongest in the regions, where the cross helicity changes the sign and becomes smallest in magnitude. Thus, our simulations provide an important opportunity to explore the regions of magnetic reconnections in nonlinear MHD.

Introduction. The concept of magnetohydrodynamic (MHD) turbulence is important to explain a great number of plasma phenomena observed in fundamental astrophysics and applied physics fusion plasma. Studies of MHD turbulence are aimed to achieve the common view on excitation, nonlinear transport and dissipative mechanisms. Still there are many aspects that need to be clarified. Magnetic reconnection is a crucial physical phenomenon that significantly affects the energy release during many astrophysical processes, such as solar flares, aurora in the Earth's magnetosphere, etc. This is the topic of the present paper.

A simple MHD model for a steady state magnetic reconnection was suggested by Parker [1]. In the presence of turbulence, the reconnection rate may be drastically changed in contrast to the laminar case. The primary effect of turbulence is to enhance the effective transport. At large magnetic Reynolds numbers, which are ubiquitous in astrophysical phenomena, the turbulent magnetic diffusivity in the magnetic induction is much larger than the molecular counterpart, such as the Spitzer diffusivity. Through this effective diffusivity turbulence is expected to contribute to the enhancement of magnetic reconnection.

However, in the presence of a broken mirror symmetry caused by a kind of external helical forcing, we have other important turbulence effects. In addition to the enhanced transport, suppression of transport may be also caused by turbulence. The total amount of the cross helicity (velocity–magnetic-field correlation), which represents the asymmetry between the directions parallel and antiparallel to the magnetic field, is an inviscid invariant of the MHD equations as well as the counterparts of the MHD energy and magnetic helicity. The basic role of cross helicity in magnetic induction is to suppress the turbulent magnetic diffusivity arising from the turbulent energy [2]. Recently it was found that a weak inverse transfer of the kinetic energy toward large scales could be due to the presence of strong cross helicity at small scales [3].

It was found that in the presence of turbulent cross helicity, a dynamic balance between transport enhancement and suppression occurs [4]. These turbulence effects on transport are based on the coarse-grained view or the mean-field approach to turbulence. However, this does not mean that the dynamic-balance arguments are not relevant to full direct numerical simulations (DNSs) of the fundamental MHD equations. These basic properties of the turbulence transport are intrinsically contained in the fundamental equations of the MHD turbulence with broken symmetry. The applicability of the mean-field approach in the context of magnetic reconnection was shown by numerical

simulations of a Reynolds-averaged MHD turbulence model [5]. A subgrid-scale (SGS) turbulence model was used to investigate the contributions of the SGS turbulent energy and cross helicity to the plasmoid reconnection rate [6].

If the cross helicity density changes its sign in a spatiotemporal region at some scale, there is no transport suppression in this region because of the vanishing cross helicity. Rather we have a transport enhancement originating from the turbulent energy. This lack of transport suppression readily leads to a maximized magnetic reconnection due to a localized enhanced turbulent diffusivity [4]. Once magnetic reconnection is induced at some point with the associated local out- and in-flows, a quadrupole spatial distribution of the cross helicity is reproduced and sustained. Then a quadruple cross helicity configuration with the reversal of the cross helicity sign at the symmetric points, preferable for the enhanced magnetic reconnection, is likely to be further reinforced [7]. This suggests strong correlations between the regions of cross helicity reversal and those of strong reconnections with non-zero cross helicity.

Turbulent magnetic diffusivity or resistivity in the correlated (non-zero cross helicity) MHD turbulence has been investigated for a long time. Using numerical simulations of the eddy-damped quasi-normal Markovianised (EDQNM) approximation closure equation, it was shown that the sign of the cross helicity reversed at the dissipation scale with the equipartition between the kinetic and magnetic energies [8]. With the aid of direct numerical simulations of the decaying two-dimensional MHD flows, the spectral properties of MHD turbulence with a non-zero cross helicity were investigated and the current sheet formation at the very small scales was reported [9]. Field theory calculations for MHD turbulence with a large cross helicity were performed in [10].

The purpose of this paper is to demonstrate that the scenario for reconnection of the magnetic field is realized under the conditions of homogeneous isotropic forced MHD turbulence. We have found that, starting with a small scale in the dissipative interval, isolated reconnection structures are observed which are well correlated with regions, where cross helicity changes its sign.

1. Direct numerical simulation of MHD turbulence with cross helicity injection. We solve the dimensionless equations of incompressible magnetohydrodynamics

$$\partial_t \mathbf{u} + (\mathbf{u}\cdot\nabla)\mathbf{u} = (\mathbf{b}\cdot\nabla)\mathbf{b} + {\mathrm{R_u}}^{-1}\,\nabla^2\mathbf{u} + \mathbf{F}_u - \nabla p, \tag{1}$$

$$\partial_t \mathbf{b} + (\mathbf{u}\cdot\nabla)\mathbf{b} = (\mathbf{b}\cdot\nabla)\mathbf{u} + \mathrm{Rm}^{-1}\nabla^2\mathbf{b} + \mathbf{F}_b, \tag{2}$$

$$\nabla\cdot\mathbf{u} = \nabla\cdot\mathbf{b} = 0, \tag{3}$$

where $\mathbf{u}$, $\mathbf{b}$, p are, respectively, the velocity, magnetic and normalized pressure fields, $\mathrm{R_u}$ and Rm are the kinetic and magnetic Reynolds numbers. $\mathbf{F}_u$ and $\mathbf{F}_b$ are the external large-scale forces.

The equations are numerically integrated using the pseudospectral code Tarang [11]. It is a general-purpose flow solver for turbulence and instability studies. Tarang scales nearly up to 196608 cores [12]. Helical MHD turbulence can be studied using implemented features: forcing, spectra, fluxes and mode-to-mode transfer of kinetic, magnetic and cross helicity [13]. For the purpose of this work, we introduced random forces which control the total energy injection ε and cross helicity ε_c rates. In the Fourier space, their expressions can be written in the following form

$$\mathbf{F}_u(\mathbf{k}) = ((\varepsilon-\varepsilon_c)^{1/2}\mathbf{e}_u(\mathbf{k}) + \varepsilon_c^{1/2}\mathbf{e}_c(\mathbf{k})), \tag{4}$$

$$\mathbf{F}_b(\mathbf{k}) = ((\varepsilon-\varepsilon_c)^{1/2}\mathbf{e}_b(\mathbf{k}) \pm \varepsilon_c^{1/2}\mathbf{e}_c(\mathbf{k})), \tag{5}$$

where $\mathbf{e}_*$ is a random vector with $|\mathbf{e}_*| = (\Delta t N_f)^{-1/2}$, where subscript '*' stands for the subscripts u, b and c. Here Δt is the time step, N_f is the number of modes where forcing is applied. A more general form of Eqs. (4) and (5) and their detailed derivations can be

found in [14]. In our forcing parametrization, $\varepsilon \geq \varepsilon_c \geq 0$. The sign of the injected cross helicity is controlled by the choice of sign in Eq. (5).

2. Results. Simulations were performed in a triply periodic domain of size 2π on a grid 512^3. Forcing acts in a range of scales $1 < |\mathbf{k}| \leq 3$. We fixed $\varepsilon = 2$ with which we have achieved $\mathrm{Re} = \mathrm{Rm} \approx 2094$. It corresponds to a Kolmogorov's dissipation wave number $k_d \approx 100$. The parameter $C = \varepsilon_c/\varepsilon$ was varied to determine the effect of cross helicity. The simulation was initialized with a random distribution of weak kinetic and magnetic fields. It took about 30 units of time to reach a quasi-stationary regime of MHD turbulence. The data of the next 10 units of time are taken for evaluating the averaged energy and cross helicity spectra for three values of $C = 0$, 0.3, 0.6 (see Figs. 1 and 2).

The total energy spectra in Fig. 1(a) get steeper with the increase of C. The energy is gradually accumulated at large scales because its transfer in the inertial range is suppressed by the cross helicity. One can see that the spectra cross each other at a scale $k \approx 20$. This means that the dissipation scales are larger for a larger C. Such behavior was also observed in the MHD turbulence simulated with the shell models [15]. Fig. 1(b) shows separated energy spectra for the Elsässer variables $\mathbf{Z}^{\pm} = \mathbf{u} \pm \mathbf{b}$. We have found that E^+ increases, but E^- decreases compared to the $C = 0$ case. Note that E^- has a peak at the beginning of the dissipation scales. It can be explained by a fast drop of E^+ which works as advection for E^-.

The cross helicity also increases with C, but the slope does not change significantly (see Fig. 2(a)). One can observe an abrupt fall of $|H_c(k)|$ near $k_r \approx 70$. It corresponds to a change of the sign which is better visible in the distribution of the relative cross helicity $H_c^r = H_c/(E_u E_b)^{1/2}$ (Fig. 2(b)). We note this remarkable feature of H_c that changes its sign and reaches rather high relative values at the dissipative scales. The sign reversal by H_c reflects a crossing of E^+ and E^- since $H_c = E^+ - E^-$. It may happen due to a tendency of E^+ to steepen and of E^- to flatten with increasing C.

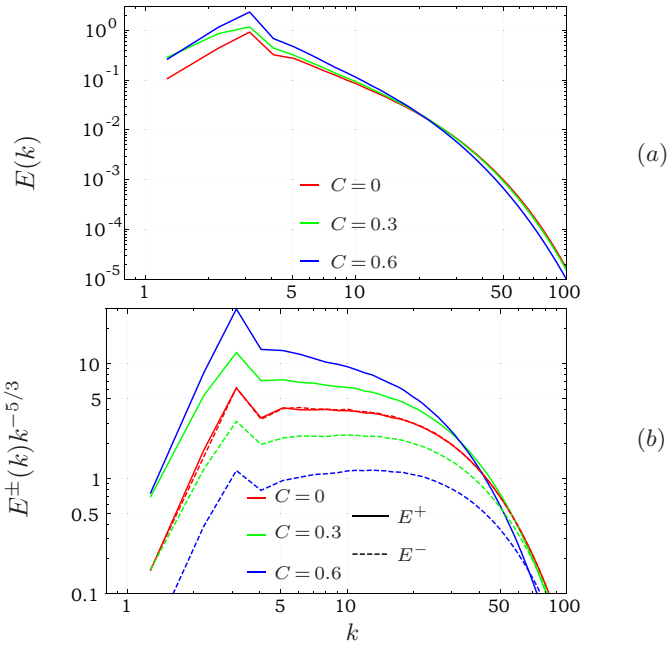

Fig. 1. MHD simulations with different cross helicity forcing ($C = 0$, 0.3, 0.6): (a) total energy spectra; (b) compensated energy spectra of Elsässer variables.

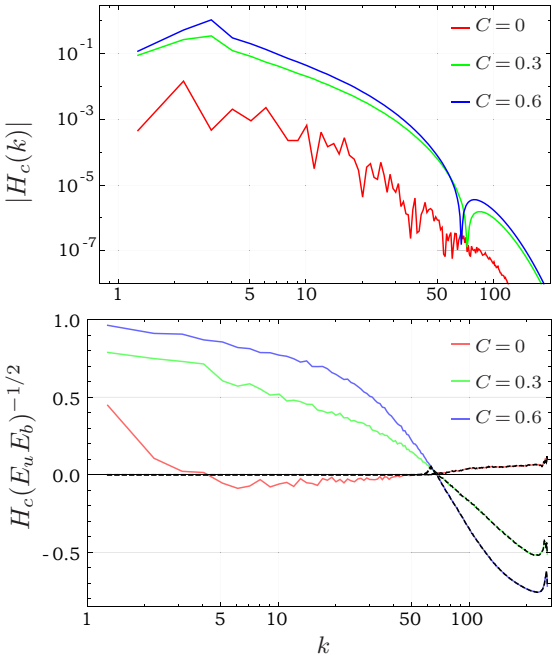

Fig. 2. MHD simulations with different cross helicity forcing ($C=0$, 0.3, 0.6): (a) absolute value of cross helicity spectra; (b) relative spectra of cross helicity. Dashed lines represent remnants after high pass filtering.

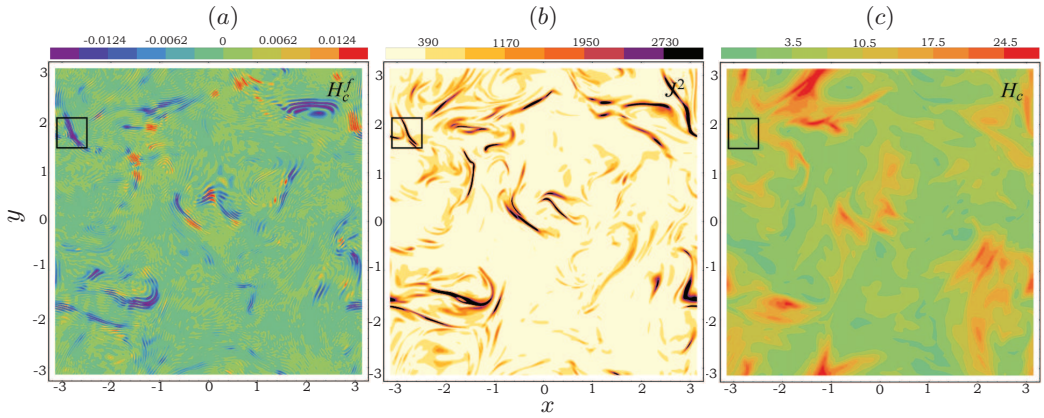

Fig. 3. MHD simulation with $C = 0.6$, density plots at a horizontal cross section at $z=1.78$ of : (a) small scales of cross helicity; (b) dissipation rate of the total magnetic field; (c) total cross helicity. The distributions are shown in a range limited by $\pm\frac{1}{10}$ of the maximum absolute value of H_c^f for panel (a) and by $\pm\frac{1}{2}$ of the maximum value of $|J^2|$ for panel (b).

We extract small scale kinetic and magnetic fields by applying a Gaussian filter in the Fourier space as

$$\mathbf{x}^f(\mathbf{k}) = \mathbf{x}(\mathbf{k})\mathrm{e}^{-(k_r-k)/k_f} \tag{6}$$

for all $k < k_r$ with the filter width $k_f = 3$. An instantaneous spacial cross-section distribution of the small-scale cross helicity $H_c^f = \mathbf{u}^f \cdot \mathbf{b}^f$ is shown in Fig. 3(a), and that of the magnetic dissipation $|\mathbf{J}|^2$ is shown in Fig. 3(b). In Fig. 3(a), we observe strong peaks of negative cross helicity (opposite to the sign of the injected H_c). H_c is localized in the filamentary structures. The regions of the negative H_c are strongly correlated

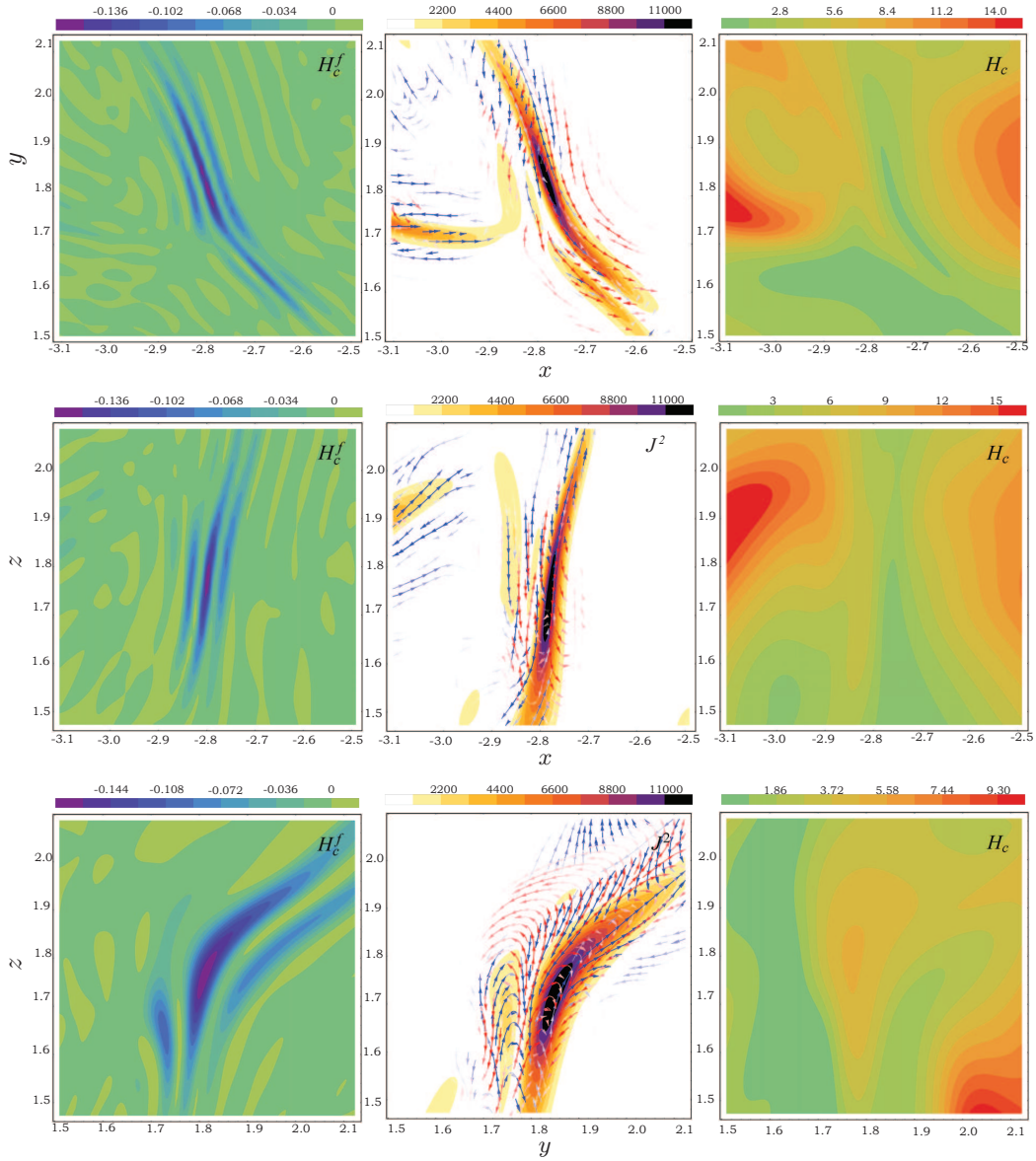

Fig. 4. MHD simulation with $C = 0.6$, at the cross-sections xOy, yOz and xOz (from top to bottom): (left column) density plots of H_c^f; (middle column) streamlines of small scale magnetic field (red) and velocity field (blue), and density plots of magnetic dissipation $|\mathbf{J}|^2$; (right column) density plots of cross helicity H_c in the vicinity of the selected reconnection zone enclosed by rectangular boxes in Fig. 3.

with those with the strong $|\mathbf{J}|^2$ (see Fig. 3(b)), which describes a magnetic dissipation and reconnection. Fig. 3(c) shows the H_c distribution of all scales that are dominated by large-scale forcing.

We consider in details an anisotropic structure of an individual reconnection. Fig. 4 displays the distribution of small scale kinetic and magnetic fields, the total H_c and $|\mathbf{J}|^2$ in orthogonal cross-sections are enclosed by rectangular boxes (upper left regions) in Fig. 3.

Conclusions. We numerically investigated the distribution of cross helicity in MHD turbulence that was forced by energy and cross helicity injections at large scales. In the dissipation range, we observed a significant level of the relative cross helicity, as well as reversal of cross helicity as we traversed from large to small scales. This feature was reported earlier in [16], but it has not been analyzed in detail. The presence of relatively high levels of relative cross helicity in the dissipation range is in marked contrast to the vanishing kinetic helicity in the dissipative range of hydrodynamic turbulence. This difference is due to the difference in order of derivatives of kinetic helicity and cross helicity in the dissipation range.

More importantly, we observed that magnetic reconnections occurred in the regions, where a small scale negative cross appeared. Also, the length scales of the cross helicity and magnetic reconnection are very similar. If we change the scales (or corresponding modes in the shell model), this correspondence between the vanishing cross helicity and the high dissipation becomes less clear. This issue merits further investigation.

At a scale other than the cross helicity reversal, the cross helicity density in turbulence is in general finite and not null. The scale dependence of the spatiotemporal distributions of cross helicity and magnetic dissipation at very high Reynolds numbers can be effectively obtained using shell models of MHD turbulence [17, 18].

Acknowledgments. We are grateful to Professor Franck Plunian for his interest in the subject and for useful comments. The developed mathematical model and the performed numerical simulations were supported by the Department of Science and Technology, India (INT/RUS/RSF/P-03) and by the Russian Science Foundation (RSF-16-41-02012) for the Indo-Russian project. Computational resources were provided by Shaheen II of the Supercomputing Laboratory at King Abdullah University of Science and Technology (KAUST) under project K1052. Theoretical studies of magnetic reconnection problems were also supported by the Japan Society for the Promotion of Science (JSPS) Grants-in-Aid for Scientific Research 18H01212. We thank the Scientific Committee of the Third Russian Perm Conference on Magnetohydrodynamics for organizing a warm atmosphere and stimulation discussions.

References

[1] E.N. Parker. Sweet's mechanism for merging magnetic fields in conducting fluids. *Journal of Geophysical Research*, vol. 62 (1957), no. 4, pp. 509–520.

[2] N. Yokoi. Cross helicity and related dynamo. *Geophysical and Astrophysical Fluid Dynamics*, vol. 107 (2013), no. 1-2, pp. 114–184.

[3] A. Brandenburg and S. Oughton. Cross-helically forced and decaying hydromagnetic turbulence. *arXiv e-prints 1901.05875*, (2019). Accepeted in Astr. Nach.

[4] N. Yokoi, K. Higashimori, and M. Hoshino. Transport enhancement and suppression in turbulent magnetic reconnection: A self-consistent turbulence model. *Physics of Plasmas*, vol. 20 (2013), no. 12, p. 122310.

[5] K. Higashimori, N. Yokoi, and M. Hoshino. Explosive turbulent magnetic reconnection. *Phys. Rev. Lett.*, vol. 110 (2013), p. 255001.

[6] F. Widmer, J. Bchner, and N. Yokoi. Characterizing plasmoid reconnection by turbulence dynamics. *Physics of Plasmas*, vol. 23 (2016), no. 9, p. 092304.

[7] N. Yokoi and M. Hoshino. Flow–turbulence interaction in magnetic reconnection. *Physics of Plasmas*, vol. 18 (2011), no. 11, p. 111208.

[8] R. Grappin, A. Pouquet, and J. Léorat. Dependence of mhd turbulence spectra on the velocity field-magnetic field correlation. *Astronomy and Astrophysics*, vol. 126 (1983), no. 1, pp. 51–58.

[9] H. Politano, A. Pouquet, and P.L. Sulem. Inertial range and resistive instabilities in two-dimensional magnetohydrodynamic turbulence. *Physics of Fluids B*, vol. 1 (1989), no. 12, pp. 2330–2339.

[10] M.K. Verma. Statistical theory of magnetohydrodynamic turbulence: recent results. *Phys. Rep.*, vol. 401 (2004), no. 5, pp. 229–380.

[11] M.K. Verma, *et al.* Benchmarking and scaling studies of pseudospectral code Tarang for turbulence simulations. *Pramana – Journal of Physics*, vol. 81 (2013), no. 4, pp. 617–629.

[12] A.G. Chatterjee, *et al.* Scaling of a fast fourier transform and a pseudo-spectral fluid solver up to 196608 cores. *Journal of Parallel and Distributed Computing*, vol. 113 (2018), pp. 77–91.

[13] R. Stepanov, *et al.* Direct numerical simulation of helical magnetohydrodynamic turbulence with tarang code. In *2017 Ivannikov ISPRAS Open Conference (ISPRAS)* (2017), pp. 90–96.

[14] V. Titov. Direct numerical simulation of homogeneous isotropic cross-helical magnetohydrodynamic turbulence. *Computational Continuum Mechanics*, vol. 12 (2019), no. 1, pp. 5–16.

[15] I.A. Mizeva, R. Stepanov, and P.G. Frik. The cross helicity effect on cascade processes in MHD turbulence. *Dokl. Phys.*, vol. 54 (2009), no. 2, pp. 93–97.

[16] M.E. McKay, *et al.* Comparison of forcing functions in magnetohydrodynamics. *Phys. Rev. Fluids*, vol. 2 (2017), p. 114604.

[17] R. Stepanov, P. Frick, and I. Mizeva. Cross helicity and magnetic helicity cascades in MHD turbulence. *Magnetohydrodynamics*, vol. 49 (2013), no. 1–2, pp. 15–21; DOI: 10.22364/mhd.49.1-2.3.

[18] P. Frick and R. Stepanov. Long-term free decay of MHD turbulence. *EPL (Europhysics Letters)*, vol. 92 (2010), p. 34007.

Received 24.01.2019